EVOLUTION & DEVELOPMENT 14:5, 450–463 (2012)
DOI: 10.1111/j.1525-142X.2012.00565.x

Hox gene expression in the harvestman *Phalangium opilio* reveals divergent patterning of the chelicerate opisthosoma

Prashant P. Sharma,[a,b,*] Evelyn E. Schwager,[b] Cassandra G. Extavour,[b] and Gonzalo Giribet[a,b]

[a] Museum of Comparative Zoology, Harvard University, 26 Oxford Street, Cambridge, MA, 02138, USA
[b] Department of Organismic and Evolutionary Biology, Harvard University, 26 Oxford Street, Cambridge, MA, 02138,USA

[*] Author for correspondence (email: psharma@fas.harvard.edu)

SUMMARY Among chelicerates, Hox gene expression has only been investigated in representatives of two arachnid orders to date: Acari (mites and ticks) and Araneae (spiders). Limited data are available for the "primitive" arachnid orders, such as Scorpiones (scorpions) and Opiliones (harvestmen). Here, we present the first data on Hox gene expression in the harvestman *Phalangium opilio*. Ten Hox genes of this species were obtained from a de novo assembled developmental transcriptome using the Illumina GAII platform. All 10 genes are expressed in characteristic Hox-like expression patterns, and the expression of the anterior and central Hox genes is similar to those of other chelicerates. However, intriguingly, the three posteriormost genes—*Ultrabithorax*, *abdominal-A*, and *Abdominal-B*—share an identical anterior expression boundary in the second opisthosomal segment, and their expression domains extend through the opisthosoma to the posterior growth zone. The overlap in expression domains of the posterior Hox genes is correlated with the absence of opisthosomal organs posterior to the tubular tracheae, which occur on the second opisthosomal segment. Together with the staggered profile of posterior Hox genes in spiders, these data suggest the involvement of *abdominal-A* and *Abdominal-B* in the evolution of heteronomous patterning of the chelicerate opisthosoma, providing a mechanism that helps explain the morphological diversity of chelicerates.

INTRODUCTION

The morphological diversity of arthropods has been attributed to their segmented bauplan and its modularity through the process of tagmatization, whereby groups of adjacent segments evolve in concert to achieve morphological and functional distinction from other groups of segments (Cisne 1974). Different groups of segments have evolved in concert and achieved a variety of functions in the course of tagmosis, facilitating the concentration of physiological functions in different body regions and favoring adaptations to broad arrays of ecological niches and environments. Because the Hox genes play important roles in conferring segmental identity, it is likely that these genes were a driving force in the evolution of tagmata (e.g., Lewis 1978; Denell et al. 1981; Carroll 1995; Popadic et al. 1998; Hughes and Kaufman 2002a). Loss or gain of Hox gene function results in homeotic transformations, whereby the fate of one or more segments is altered, irrespective of tagmatic boundaries (e.g., Denell et al. 1981; Pultz et al. 1988; Angelini et al. 2005; Liubicich et al. 2009; Khadjeh et al. 2012).

Investigations of how Hox genes engender evolutionary lability have prompted surveys of this gene cluster across the arthropod phylogenetic tree (reviewed by Hughes and Kaufman 2002a; Angelini et al. 2005; Brena et al. 2006; Jager et al. 2006; Janssen and Damen 2006; Manuel et al. 2006). In many cases, there is strong evidence that changes in Hox gene expression domains underlie the morphological evolution of specific segments. One of the most compelling such cases comprises the correlation of the anterior expression boundary of *Ultrabithorax/abdominal-A* with the boundary between the maxillipeds and thoracopods (locomotory appendages) in crustaceans (Averof and Patel 1997). A knockdown of *Ultrabithorax* (*Ubx*) has been shown to result in additional maxillipeds in the amphipod crustacean *Parhyale hawaiensis* (Liubicich et al. 2009). Conversely, ectopic *Ubx* expression results in transformation of maxillipeds to thoracopods (Pavlopoulos et al. 2009). As another example, *Ubx* and *abdominal-A* (*abd-A*) are known to inhibit limb growth in the abdomen of several insects by repressing the expression of *Distal-less* (González-Reyes and Morata 1990; Mann and Hogness 1990; Ueno et al. 1992; Vachon et al. 1992; Zheng et al. 1999; Lewis et al. 2000). No functional studies have been conducted in the remaining group of mandibulates, the myriapods, but gene expression studies in two centipedes (Hughes and Kaufman 2002b; Brena et al. 2006) and a millipede (Janssen and Damen 2006) have demonstrated coincident or nearly coincident boundaries of *Ubx* and *abd-A*

in both lineages, which correlates with the absence of tagmosis in the homonomous trunk of myriapods (Hughes and Kaufman 2002b). Thus, changes in Hox gene expression can underlie the degree of heterogeneity within tagmata.

An unexplored area of Hox gene study is their role in the evolution of the posterior tagma (or opisthosoma) of Chelicerata. The chelicerate anterior tagma (prosoma) typically consists of the ocular and six appendage-bearing segments. The prosoma is a highly conserved feature across the chelicerates (barring Pycnogonida (sea spiders), which have an autapomorphic appendage pair called the ovigers, and four to six pairs of walking legs; Jager et al. 2006; Brenneis et al. 2008). Within arachnids, the composition of the prosoma is invariable; it is the appendages that have undergone significant evolutionary modifications in various lineages. By contrast, the chelicerate opisthosoma is highly variable in four major morphological respects: segment number, segment allometry, opisthosomal organs, and embryonic opisthosomal appendages. First, the number of segments ranges from nearly nonexistent in some sea spiders, to two true segments in some mites, to 13 in scorpions, with one of those seen only in embryonic development (Dunlop 1998; Grbic et al. 2011). Second, the allometry of corresponding segmental sternites and tergites is variable: for example, the second and third opisthosomal sternites are miniaturized in Uropygi (vinegaroons; Shultz 1993). Third, there is variation in the number and type of opisthosomal organs. For example, Opiliones have a single pair of tubular tracheae, whereas Xiphosura have a pair of reduced appendages (chilaria) and five pairs of book gills (Damen et al. 2002). Finally, the number of embryonic opisthosomal appendages ranges from none in mites and Opiliones to seven pairs in Scorpiones (Farley 2001). In the case of scorpions and the extinct eurypterids, the opisthosoma is further subdivided into the characteristic mesosoma and metasoma. It follows that the activity and expression boundaries of posterior Hox genes across Chelicerata are of interest in the context of evolutionary developmental biology.

Expression data for some anterior Hox genes were generated for pycnogonids in the effort to settle disputes over the homology of the sea spider chelifore (Maxmen et al. 2005; Jager et al. 2006; Brenneis et al. 2008), but these studies did not address the expression of posterior Hox genes in the opisthosoma (note that the inclusion of pycnogonids in Chelicerata remains in contention; Giribet et al. 2001; Dunn et al. 2008; Regier et al. 2008, 2010; Hejnol et al. 2009; Meusemann et al. 2010; see a recent review in Giribet and Edgecombe 2012). *Ubx* expression domains have been observed in a scorpion and a xiphosuran (Popadic and Nagy 2001). Somewhat more data are available for acariform mites (Telford and Thomas 1998a, 1998b; Telford 2000), but expression domains of the posterior Hox genes *Ultrabithorax*, *abd-A*, and *Abdominal-B* (*Abd-B)* in mites are entirely unknown.

The complete suite of posterior Hox gene domains in chelicerates is presently reported only for three species of spiders (Damen et al. 1998; Damen and Tautz 1998; Abzhanov et al. 1999; Schwager et al. 2007; Khadjeh et al. 2012). In all spiders examined to date, the anterior boundaries of the genes *Ubx*, *abd-A*, and *Abd-B* have a "staggered" profile, that is, the anterior boundary of each is displaced from the consecutive gene by one to two segments. These boundaries correlate with the apomorphic opisthosomal organ configuration of araneomorph (i.e. derived) spiders: in the species *Achaearanea tepidariorum* and *Cupiennius salei*, the second opisthosomal segment (O2) bears a pair of book lungs and contains the anterior boundary of *Ubx*; O3 bears a pair of tubular tracheae and contains anterior boundary of *abd-A*; and O4 and O5 each bear pairs of spinnerets, with expression of *Abd-B* commencing in O4 (Damen et al. 1998; Damen and Tautz 1999). However, it is difficult to generalize these expression domains for other chelicerate orders that have differing sets of opisthosomal organs and segments (e.g. scorpions), or lineages that have lost opisthosomal segmentation altogether (e.g. mites).

In order to test the hypothesis that Hox gene activity varies with the morphological disparity of various chelicerate orders, we examined gene expression of all 10 Hox genes in the harvestman *Phalangium opilio*. Although the prosoma of the harvestmen is similar to that of the spiders, the opisthosoma is markedly different, lacking the diminutive pedicel (the stalk between the two tagmata derived from the first opisthosomal segment in spiders; in harvestmen, the two tagmata are fused), as well as opisthosomal appendages during embryogenesis. Additionally, in contrast to the four pairs of opisthosomal organs in spiders, harvestmen bear only a single pair of tubular tracheae, which terminate in a pair of spiracles on the second opisthosomal segment. We therefore compared differences in gene expression in spiders and the harvestman to determine whether their respective morphologies are correlated with Hox expression domains.

MATERIALS AND METHODS

Phalangium opilio cultivation and embryo fixation

Adults of the synanthropic *P. opilio* (Arachnida, Opiliones, Eupnoi, Phalangiidae) were hand collected between 9 PM and 3 AM from various sites in Weston and Woods Hole (Falmouth) Massachusetts, USA in May through October of 2009–2011. Four to five females were housed with single males following the setup of Allard and Yeargan (2005). Animals were fed ad libitum with freshly killed *Drosophila melanogaster*. Clutches (25–120 eggs/clutch) deposited under florist's foam or on the sides of the container were collected and transferred to a 30°C incubator. Stages were determined by dechorionating one to two eggs from a single

clutch in weak bleach solution and observing embryos under a light microscope (stages are roughly synchronized within a clutch). Fixation was conducted by modifying the spider protocol of Akiyama-Oda and Oda (2003) as follows: eggs were dechorionated in weak bleach solution for 4–5 min, followed by washes with distilled water. Bleach-perforated chorions were either removed by hand or by a quick agitation step on a vortexer. The embryos were then fixed in a 1:1 mixture of heptane and 4% formaldehyde in 1× PEMS with agitation on a platform shaker overnight at room temperature, subsequently rinsed with 1× PEMS + Tween-20 0.1% (PEMS-Tween), gradually dehydrated in methanol (25%, 50%, 75% MeOH in PEMS-Tween, each for 10 min) and stored at −20°C in 100% methanol.

Gene identification and whole mount in situ hybridization

RNA was extracted from a range of embryonic stages using Trizol (Invitrogen, Carlsbad, CA, USA) and first strand cDNA synthesis was performed using SuperScriptIII (Invitrogen). A developmental transcriptome of *P. opilio* was generated by sequencing this cDNA in a single flowcell on an Illumina GAII platform, using paired-end 150-bp-long reads. Thinning was performed using 0.0496 as the limit (based on Phred quality scores), and the resulting quality of the thinned reads was visualized using FastQC (http://www.bioinformatics.bbsrc.ac.uk/projects/fastqc/). After thinning, only those terminal bases with a Phred quality score under 30 were trimmed. Assembly was conducted using CLC Genomics Workbench 4.6.1 (CLC bio, Aarhus, Denmark). Fragments of 10 Hox genes, as well as the segment polarity gene *engrailed* (*en*) were identified by BLAST in single copy; sequences ranged in length from 441 to 2553 bp. The full transcriptome will be described and characterized elsewhere (Sharma and Giribet, unpublished data).

To confirm gene identity, phylogenetic analysis of Hox gene amino acid sequences was conducted as follows: Hox gene amino acid sequences of chelicerates and mandibulates were aligned using MUSCLE v. 3.6 (Edgar 2004) and culled to 68 conserved, adjacent positions using GBlocks v. 0.91b (Castresana 2000). Maximum likelihood analysis was performed using RAxML v. 7.2.7 (Stamatakis 2006) on 12 CPUs of a cluster at Harvard University, FAS Research Computing (odyssey.fas.harvard.edu). For the maximum likelihood search, a Jones-Taylor-Thornton model of sequence evolution with corrections for a discrete gamma distribution (JTT + Γ; Jones et al. 1992; Yang 1996) was specified, and 50 independent searches were conducted. The results are illustrated in Supporting Information Fig. S1 and the alignments are available in a supplementary text file. Sequences of all genes are deposited in GenBank under accession numbers HE805493–HE805502.

Templates for riboprobe synthesis were generated as described by Lynch et al. (2010): Genes were amplified by PCR using gene-specific primers (GSP) with an added linker sequence (5′-ggccgcgg-3′ for the forward primer end and 5′-cccggggc-3′ for the reverse primer). A T7 polymerase binding site for antisense or sense probe synthesis was generated in a second PCR using the forward or reverse GSP and a universal primer binding to the 3′ or 5′ linker sequence with an added T7 binding site, respectively. GSPs were designed from the identified transcriptomic assembly. A list of the primers used for generating sense and antisense probes is provided in Supporting Information Table S1. Probe synthesis and in situ hybridization followed the spider protocols for *C. salei* (Prpic et al. 2008). The staining reactions for detection of transcripts lasted between 20 min and 6 h at room temperature. Embryos were subsequently rinsed with 1× PBS + Tween-20 0.1% to stop the reaction, counterstained with Hoechst 33342 (Sigma, St. Louis, MO, USA) 10 μg/ml to label nuclei, postfixed in 4% formaldehyde, and stored at 4°C in glycerol. Embryos were mounted in glycerol and images were captured using an HrC AxioCam and a Lumar stereomicroscope driven by AxioVision v. 4.8.2 (Zeiss, Oberkochen, Germany).

RESULTS

Overview of embryogenesis

Embryonic development of Opiliones, and specifically within the suborder Eupnoi (which includes *P. opilio*), has been well characterized by Juberthie (1964) and is comparable to that of araneomorph spiders (Foelix 1996). To facilitate comparability, we follow the staging system established by Juberthie (1964). The first visible morphological structure of the future germ band is the cumulus (or *masse génitale*, *sensu* Juberthie 1964), which undergoes migration and establishes the dorsoventral (DV) axis, as in spiders (Akiyama-Oda and Oda 2003). A diffuse germ disk then elongates along the AP axis to form a germ band with six segments on the opposite side of the egg from the site of cumulus migration. The six segments correspond to the prosomal appendage-bearing segments (Fig. 2, A and B; Ch = chelicera-bearing segment; Pp = pedipalp-bearing segment, and leg-bearing segments L1–L4). The segments then form pairs of limb buds and opisthosomal segments are added in succession from the posterior of the embryo (*métamérisation du prosoma*, *sensu* Juberthie 1964) (Fig. 2C). In Opiliones, nine opisthosomal segments are added embryonically (in the adult, 10 segments in total are present, including the telson) before the embryo undergoes inversion (a process whereby the germ band splits along the ventral midline, in many spiders and

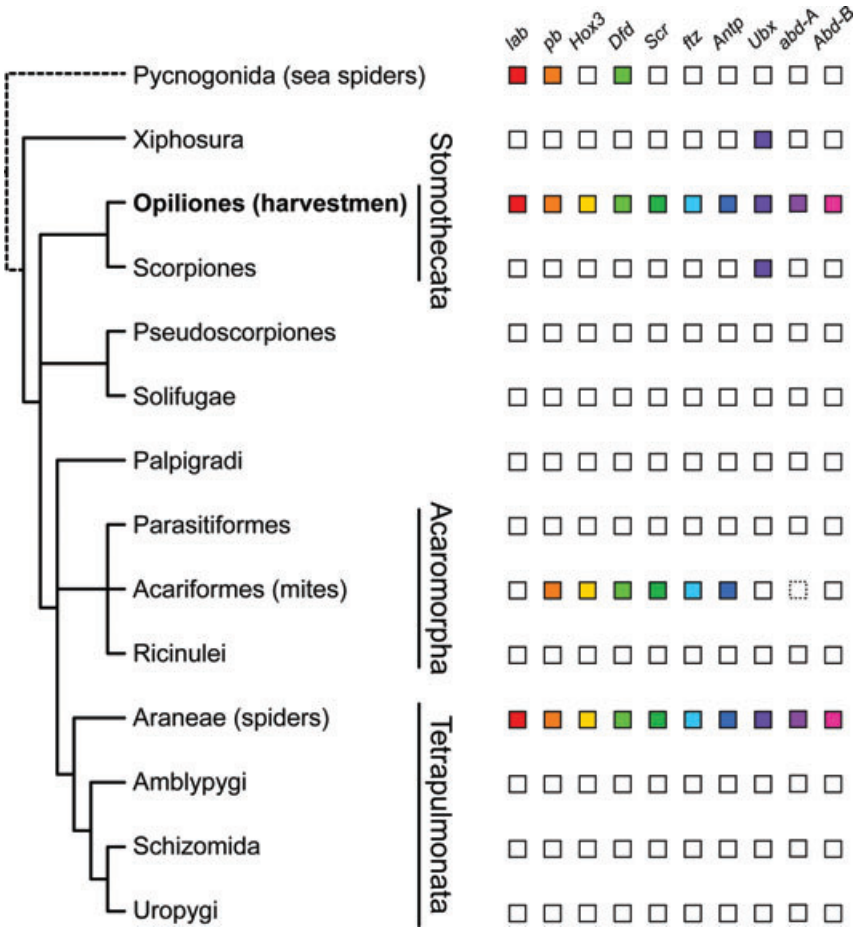

Fig. 1. Phylogeny of Chelicerata indicating relationships among orders and known Hox gene expression patterns. Boldface text indicates lineage for which Hox gene expression has been investigated in the present study. Parenthetical text indicates common names of lineages of interest. Broken line for Pycnogonida indicates uncertain phylogenetic placement. Colored squares indicate known gene expression pattern; white entries indicate unknown expression pattern; and dashed box for Acariformes indicates gene loss. Topology derived from Giribet et al. (2001), Shultz (2007), and Giribet and Edgecombe (2012).

myriapods; Anderson 1973). Embryogenesis results in a hatchling (*larve*, *sensu* Juberthie 1964) that closely resembles the morphology of the adult.

In contrast to spiders, no evidence of opisthosomal limb buds is ever observed in *P. opilio* (Fig. 2, B and C). In addition, prosomal appendage development is accelerated in *P. opilio* with respect to spiders (Fig. 2, D and E). A *C. salei* (spider) embryo stage with seven opisthosomal segments (Stage 11; Fig. 7 of Wolff and Hilbrant 2011) does not have podomerized (segmented) appendages; rather, it retains elongated prosomal limb buds and inversion does not occur until a later stage. By contrast, an embryo of *P. opilio* with the same number of opisthosomal segments already has fully podomerized prosomal appendages (Fig. 2E); cuticle deposition in some parts of the embryo has commenced and inversion has progressed significantly by this stage.

The prosomal appendages grow significantly in length during embryogenesis, with the longest leg pairs encircling the body completely in late stages (Juberthie 1964). There is marked fidelity of appendage allometry in the *P. opilio* embryo with respect to the adult, with the limb bud corresponding to the second (and longest) walking leg exceeding the width and length of all others in the earliest limb bud stages (Figs. 2, A and B and 3A).

Identification of *P. opilio* Hox genes

We discovered fragments of single copies of all 10 Hox genes (ranging in length from 441 to 2553 bp) from an embryonic transcriptome and confirmed their identity by phylogenetic analysis (Supporting Information Fig. S1). Next, we studied their expression in *Phalangium* embryos. As negative controls, we tested for expression of sense probes in embryos of various stages, but in all cases, only observed background staining incurred by cuticle deposition (data available upon request). To facilitate discourse, here we refer to *Antp*, *Ubx, abd-A*, and *Abd-B* as the "opisthosomal" group, and the remaining six genes as the "prosomal" group.

Expression of prosomal Hox genes

In limb bud stages, *Po-labial* (*Po-lab*) is strongly expressed in the pedipalpal and L1 segments, both in the appendages and

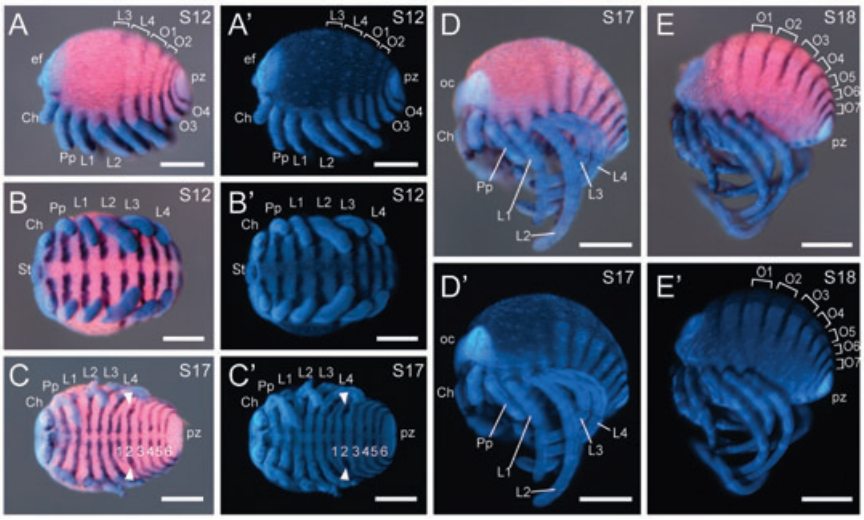

Fig. 2. Expression of the *Phalangium opilio engrailed* gene. (A) Stage 12 embryo, lateral view. Distribution of *Po-en* transcripts in the posterior part of each segment. Four opisthosomal segments are formed. (B) Same embryo as in (A) in ventral view. (C) Stage 17 embryo in ventral view. Six opisthosomal segments are formed. Spiracles appear on the O2 segment (arrowheads). For clarity, posterior boundaries of opisthosomal segments are indicated with numbers only. (D) Same embryo as in (C) in lateral view. (E) Stage 18 embryo in lateral view. Seven opisthosomal segments are formed. Note the nonspecific staining in the distal tips of the chelicerae and the bases of the appendages due to cuticle deposition in (C), (D), and (E). (A'–E') Counterstaining of embryos shown in (A–E) with Hoechst. Scale bars for all figures are 200 μm. Ch: chelicera; Pp: pedipalp; L1–L4: leg segment 1–4; O1–O7: opisthosomal segment 1–7; ef: eye field; oc: ocularium; pz: posterior growth zone.

in the ventral ectoderm. Strong expression is also detected in the ventral ectoderm of L2. Weak expression is detected in L2–L4 (Fig. 3A). In later stages, expression is retained in the pedipalps and L1, but is also observed in their corresponding endites (Fig. 3, B and C; expression in L1 endites not shown). The ventral ectoderm of the L2–L4 segments also weakly expresses *Po-lab*. *Po-lab* expression is never detected in the cheliceral segment, similar to spiders (Damen et al. 1998).

The anterior boundary of *Po-proboscipedia* (*Po-pb*) similarly occurs in the pedipalpal segment, with strong expression in the distal tips of the pedipalps and L1–L4 (Fig. 3, D and E). Expression is also observed in the ventral ectoderm of all five prosomal segments posterior to the cheliceral segment. Unlike both spider and mite *pb* homologs (Telford and Thomas 1998a; Abzhanov et al. 1999), weak expression of *Po-pb* is observed in the end of the posterior growth zone, but this expression disappears by stage 15 (Fig. 3F). The expression domain of *pb* is therefore essentially the same among the three arachnid lineages studied to date.

In limb bud stages (stage 11), *Po-Hox3* is expressed in the stomodeum; the limb buds of the pedipalps and L1–L4; the ventral ectoderm of the pedipalpal, L1–L4, and opisthosomal segments; and the posterior growth zone (Fig. 4, A–4C). Weak expression is observed in the opisthosomal segments (Fig. 4B). Within the pedipalpal and L1–L4 limb buds, expression is concentrated in a medial ring and in the distal tips (Fig. 4A). In later stages (stage 14), expression in the pedipalps and L1–L4 is restricted to the distal and internal domains, with stronger expression in the ventral ectoderm of the corresponding segments (Fig. 4D). *Po-Hox3* is also strongly expressed in the ventral ectoderm of the first two opisthosomal segments, but weakly in the posterior growth zone. Stomodeal expression is no longer observed in later stages. The expression domain of *Po-Hox3* is comparable to that of the spider *A. tepidariorum* (Abzhanov et al. 1999) and the mite *Archegozetes longisetosus* (Telford and Thomas 1998a), but no opisthosomal expression was reported in the spider *C. salei* (Damen and Tautz 1998).

Po-Deformed (*Po-Dfd*) is strongly and consistently expressed throughout the L1–L4 appendages (Fig. 4, E–H). The ventral ectoderm of the L1 segment is observed to express *Po-Dfd* (Fig. 4E). As in *C. salei* (Schwager et al. 2007) the expression of *Po-Dfd* forms rings in the legs, which are more clearly observed in older embryos (e.g. stage 17; Fig. 4, G and H). Older embryos also express *Po-Dfd* in the endites of the legs (Fig. 4G). Throughout the stages we observed, *Po-Dfd* is expressed most strongly in L2. This expression domain is similar to that observed in spiders (Damen et al. 1998; Abzhanov et al. 1999). The *Dfd* homolog of the mite *A. longisetosus* is additionally expressed throughout the opisthosoma (Telford & Thomas 1998a), but the anterior boundary of *Dfd* in all three lineages is identical.

Expression of *Po-Sex combs reduced* (*Po-Scr*) occurs mainly in the L2–L4 segments, as in spiders and mites (Telford and Thomas 1998a; Schwager et al. 2007). In limb bud stages (stage 11), expression in the L2 segment is restricted to a weak ring in the proximal-most part of the limb bud, whereas expression is stronger and localized in the distal termini of L3 and L4 (Fig. 5, A and B). Expression in L3 is consistently stronger than in L4 and forms discernible rings in the medial region of both the appendages, though the expression becomes more diffuse in later stages

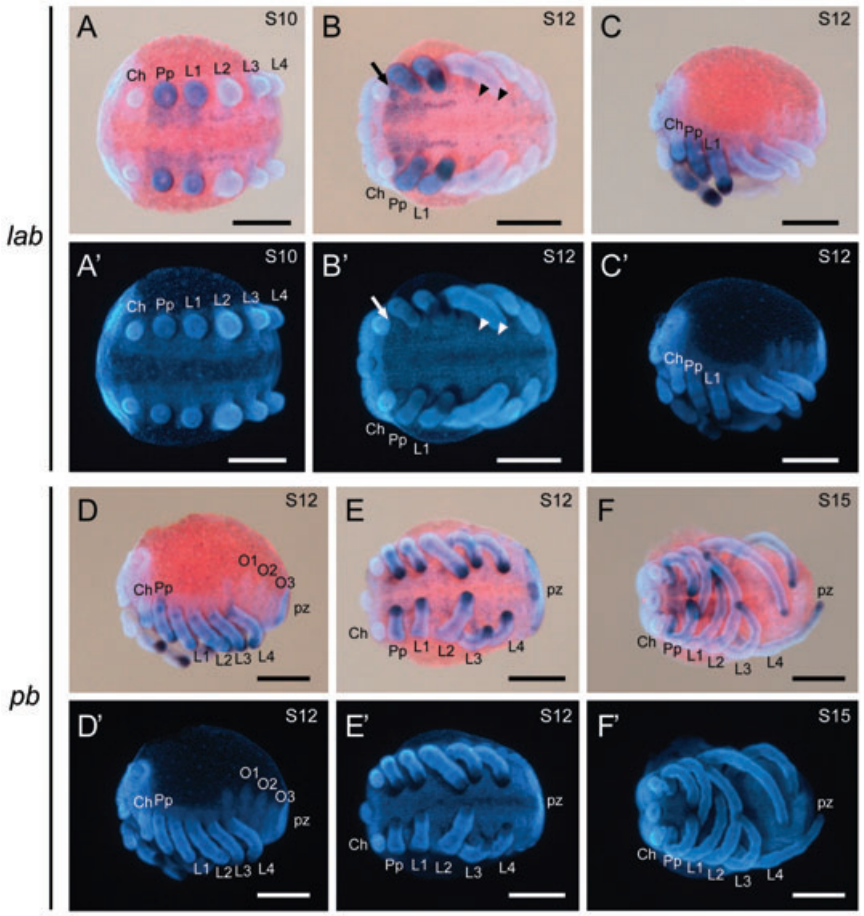

Fig. 3. Expression of the *Phalangium opilio labial* and *proboscipedia* genes. (A) Stage 10 embryo. Distribution of *Po-lab* transcripts in the pedipalpal and L1 segments, with weaker expression in L2–L4. (B) Stage 12 embryo. Endites of pedipalps and ventral ectoderm of L2–L4 express *Po-lab* (arrow and arrowheads, respectively). (C) Same embryo as in (B) in lateral view. Strong expression of *Po-lab* in the distal tips of the pedipalps and L1. (D) Stage 12 embryo in lateral view. Distribution of *Po-pb* transcripts in the pedipalps and L1–L4, with weaker expression in the ventral ectoderm of the pedipalpal, L1–L4, and opisthosomal segments. (E) Same embryo as in (D) in ventral view showing concentration of *Po-pb* in the distal tips of the pedipalps and L1–L4. (F) Stage 15 embryo. *Po-pb* is no longer expressed in the posterior growth zone. (A'–F') Counterstaining of embryos shown in (A–F) with Hoechst. Scale bars for all figures are 200 μm. Abbreviations are as in Fig. 2.

(Fig. 5, B and D). *Po-Scr* is also weakly expressed in the ventral ectoderm of L2 through L4, with stronger expression in L2 (Fig. 5C). A similar expression domain of *Scr* is observed in *A. longisetosus* (Telford and Thomas 1998a). With respect to spiders, *Po-Scr* expression resembles the union of expression domains of the two *Scr* paralogs of *C. salei*, insofar as expression is detected both in the distal portions of L3 and L4, as well as in the ventral ectoderm of these segments (as in *Scr-2*), but also in L2 (as in *Scr-1*).

Additionally, in older stages (stage 17), *Po-Scr* continues to be expressed in the L3 and L4 appendages. A paired ventral expression domain is observed in the posterior of the opisthosoma, just anterior to the posterior growth zone on either side of the ventral midline (Fig. 5D). This opisthosomal domain has not been reported in spiders or mites, and its function is presently unknown.

Prior to inversion (stage 12), *Po-fushi tarazu* (*Po-ftz*) is expressed strongly in the ventral ectoderm of the mid-prosoma through the posterior growth zone, as well as in the distal tips of the L3 and L4 appendages (Fig. 5E). As in the spider *C. salei*, the anterior boundary occurs in the L2 segment, and expression occurs prominently in the ventral ectoderm (Fig. 5F) (Damen et al. 2005). In later stages (stage 14), no expression is detected in the posterior growth zone; in the opisthosomal segments, tightly clustered and paired groups of cells express *Po-ftz* in the ventral ectoderm of O1–O4 only (Fig. 5G). *Archegozetes longisetosus ftz* is expressed in the same segments (barring O3 and O4, which are not formed at all in the mite) and with comparable decline of expression in the opisthosoma in later developmental stages (Telford 2000).

Taken together, prosomal Hox gene expression in *P. opilio* is highly similar to the expression patterns reported for spiders and mites, specifically with regard to the anterior expression borders.

Expression of opisthosomal Hox genes

In early stages (stage 12), the anterior boundary of *Po-Antp* occurs in the O1 segment, as in *A. tepidariorum* (Khadjeh et al. 2012; Fig. 6A). In subsequent stages, the *Po-Antp* expression domain expands anteriorly into the L4 segment, though the strongest expression occurs at the posterior terminus of the embryo (Fig. 6, B and C). The anteriormost

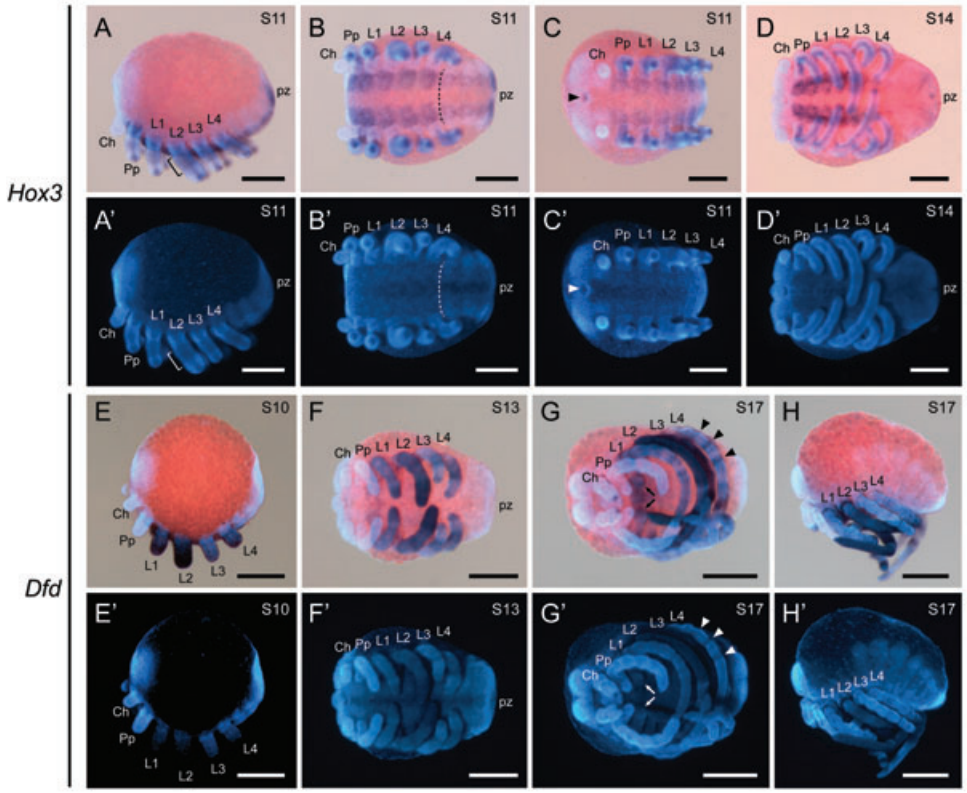

Fig. 4. Expression of the *Phalangium opilio Hox3* and *Deformed* genes. (A) Stage 11 embryo in lateral view. In the pedipalpal and L1–L4 limb buds, *Po-Hox3* is expressed in a medial ring and in the distal tips. Bracket indicates medial ring of expression in L2. (B) Same embryo as in (A) in ventral view. *Po-Hox3* is expressed in the ventral ectoderm of the prosoma and less strongly in the opisthosoma. Dashed line indicates posterior boundary of prosoma. (C) Same embryo as in (A) in anteroventral view. *Po-Hox3* is transiently expressed in the stomodeum (arrowhead). (D) Stage 14 embryo. Faint expression of *Po-Hox3* is observed in the opisthosoma. Strong expression is observed in the elongating pedipalps and L1–L4, as well as in the ventral ectoderm of the corresponding segments. (E) Stage 10 embryo in lateral view. *Po-Dfd* is expressed in L1–L4, with strong expression in L2. (F) Stage 13 embryo. *Po-Dfd* expression in L1–L4 forms rings. Ventral ectoderm of L1 additionally expresses *Dfd*. (G) Stage 17 embryo. *Po-Dfd* forms additional rings in L1–L4. Strong expression is also observed in the L1 endites (arrows). Arrowheads indicate rings of *Po-Dfd* expression in L4. (H) Same embryo as in (G) in lateral view. *Po-Dfd* is consistently expressed most strongly in L2. Note the nonspecific staining in the distal tips of the chelicerae and the bases of the appendages due to cuticle deposition. (A'–H') Counterstaining of embryos shown in (A–H) with Hoechst. Scale bars for all figures are 200 μm. Abbreviations are as in Fig. 2.

boundary of *Po-Antp* during development encompasses all of the L4 segment, in contrast to both mites—wherein the anterior boundary is restricted to the posterior half of the L4 segment (Telford and Thomas 1998a)—and spiders, wherein the anteriormost boundary occurs either in the first opisthosomal segment (in *A. tepidariorum*; Khadjeh et al. 2012) or in the posterior half of the L4 segment (in *C. salei*; Damen et al. 1998). The significance of this difference between these lineages is not known. The first and only functional studies of Hox genes in chelicerates have addressed *Antp* (as well as *Ubx* and *abd-A*) in the spider *A. tepidariorum*, and demonstrated that knockdown of *Antp* derepresses a unique pair of legs on the O1 (pregenital) segment (Khadjeh et al. 2012). Presumably, *Antp* plays a similar role in *P. opilio* with respect to conferring opisthosomal identity to the posterior segments and suppressing the expression of *Distal-less*. However, the absence of opisthosomal limb buds during embryogenesis in harvestmen and mites, as well as variability in the anterior boundary of *Antp*, renders the extrapolation of this knockdown phenotype ambiguous for other chelicerate orders.

In limb bud stages (stage 12), *Po-Ubx* is expressed from the middle of the O2 segment through the posterior growth zone, including in the ventral ectoderm of the corresponding segments (Fig. 7, A and B). However, in older stages (stage 16), *Po-Ubx* is also expressed in the genital pores, which occur on either side of the ventral midline of the second opisthosomal segment in later stages (Fig. 7, B and C); the anterior boundary of *Po-Ubx* therefore coincides with the anterior boundary of the O2 segment once the genital pores have formed

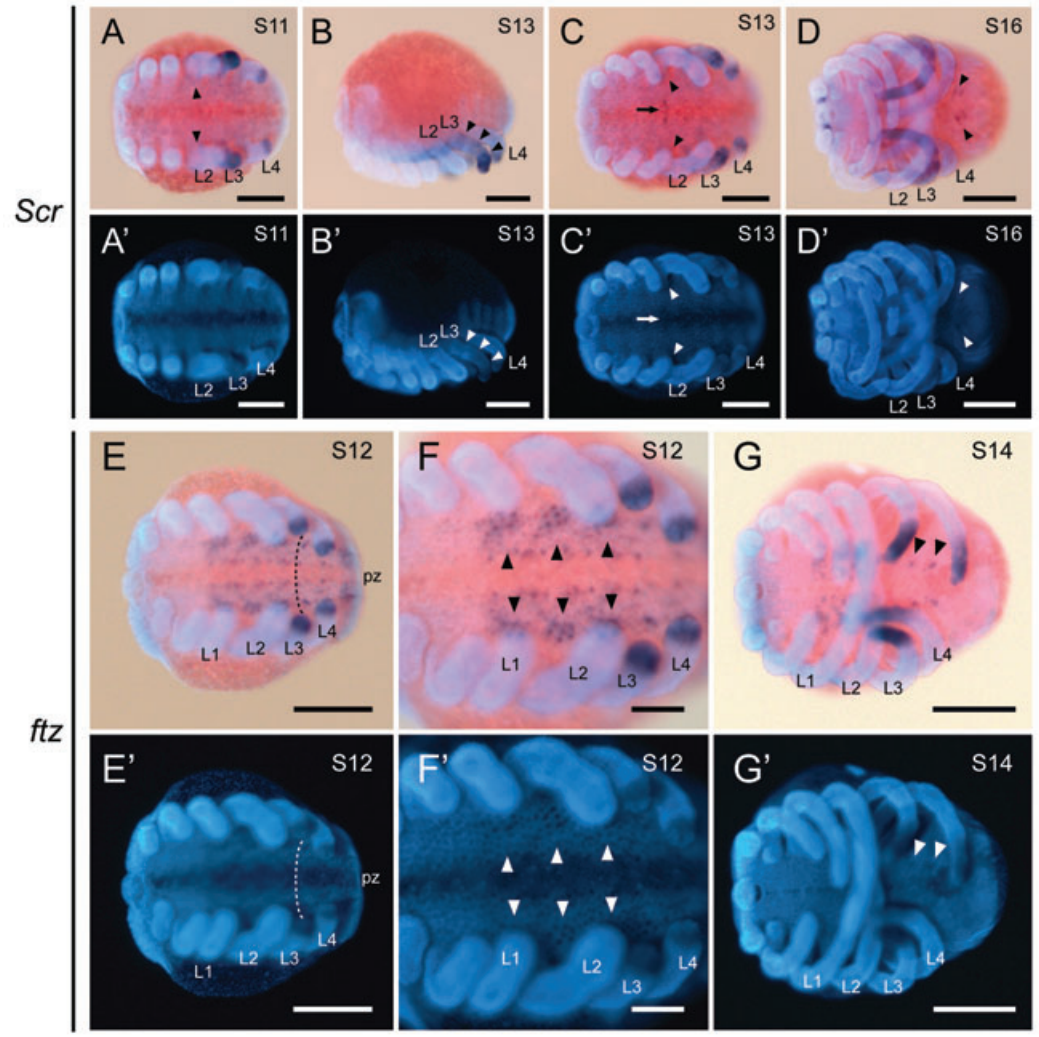

Fig. 5. Expression of the *Phalangium opilio Sex combs reduced* and *fushi tarazu* genes. (A) Stage 11 embryo. *Po-Scr* is weakly expressed in the proximal parts of the L2 limb buds (arrowheads) and the distal parts of the L3 and L4 limb buds. Expression is strongest in L3. (B) Stage 13 embryo in lateral view. *Po-Scr* expression forms rings in L3 (arrowheads). (C) Same embryo as in (B) in ventral view. *Po-Scr* expands into the ventral ectoderm at the anterior boundary of L3 (arrow). Arrowheads indicate ring of expression at the base of L2. (D) Stage 16 embryo. Rings of *Po-Scr* expression in L3 and L4 are diffuse. A pair of expression domains is observed in ventral ectoderm of the opisthosoma, just anterior of the posterior growth zone (arrowheads). Note the nonspecific staining in the distal tips of the chelicerae due to cuticle deposition. (E) Stage 12 embryo. *Po-ftz* is expressed in the distal tips of L3 and L4, and in the ventral ectoderm of all segments from L2 to the posterior growth zone. Dashed line indicates posterior boundary of prosoma. (F) Same embryo as in (E). Detail of *Po-ftz* expression in the ventral ectoderm. Arrowheads indicate invaginating cells in the L2–L4 segments. (G) Stage 14 embryo. *Po-ftz* strongly expressed in the distal parts of elongating L3 and L4. The expression domain in the ventral ectoderm of the opisthosoma is much restricted and extends only to O4. Arrowheads indicate expression domains in O3 and O4. (A'–G') Counterstaining of embryos shown in (A–G) with Hoechst. Scale bars are 100 μm for (F) and (F'), and 200 μm for all others. Abbreviations are as in Fig. 2.

(Fig. 7D). Laterally, the anterior boundary of *Po-Ubx* clearly nevertheless occurs in the posterior part of the O2 segment, retaining correspondence with the parasegmental boundary (Fig. 7E). This expression domain is essentially the same as that of the *Ubx-2* paralog in *C. salei* (Damen et al. 1998; Abzhanov et al. 1999; Schwager et al. 2007). By contrast, the anterior boundary of *Ubx* expression in both the xiphosuran and scorpion embryo is the anterior border of O2, and during development, the *Ubx* expression domain undergoes anterior shifts into the first opisthosomal (pregenital) segment (Popadic and Nagy 2001). The fate of the pregenital segment in the adult varies among the chelicerate orders, being retained as a reduced structure in spiders and xiphosurans, and lost in scorpions and harvestmen. In

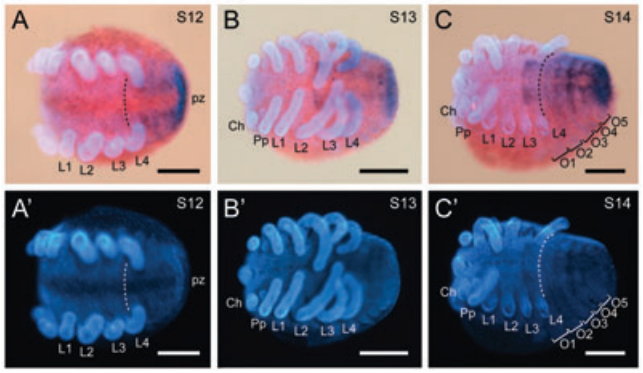

Fig. 6. Expression of the *Phalangium opilio Antennapedia* gene. (A) Stage 12 embryo. Initial expression of *Po-Antp* occurs from the O1 segment to the posterior growth zone, with strongest expression in the posterior. The anterior boundary of *Po-Antp* at this stage is diffuse. Dashed line indicates posterior boundary of prosoma. (B) Stage 13 embryo. Expression of *Po-Antp* occurs continuously from the anterior boundary of the L4 segment to the posterior growth zone. Expression is observed in the L4 appendage itself. (C) Stage 14 embryo, with legs excised for clarity. The *Po-Antp* anterior boundary is abrupt and coincident with the anterior boundary of the L4 segment. In the opisthosoma, *Po-Antp* forms distinct rings of expression that coincide with the posterior part of each opisthosomal segment, with strongest expression occurring in the posterior terminus of the embryo. Dashed line indicates posterior boundary of prosoma. (A'–C') Counterstaining of embryos shown in (A–C) with Hoechst. Scale bars for all figures are 200 μm. Abbreviations are as in Fig. 2.

Opiliones, a vestige of the pregenital segment forms the anterior part of the pregenital chamber (*arculi genitales*; Hansen and Sørensen 1904), but the segment is effectively obliterated by the anterior migration of the opisthosomal sternites toward the prosomal complex.

In an intriguing and marked departure from all chelicerate species previously studied, both *Po-abd-A* and *Po-Abd-B* are also expressed from the O2 segment through the posterior growth zone. *Po-abd-A* is expressed throughout the opisthosomal segments, but the strongest expression is detected in the posterior growth zone, the genital pore region, and in the developing spiracles (which also occur on the O2 segment, but are displaced laterally from the midline; Fig. 8, A and B). By contrast, *Po-Abd-B* is expressed in the posterior growth zone, the genital pore region, and in the ventral ectoderm (i.e. along the midline) of the opisthosomal segments (Fig. 8, C and D). No *Po-Abd-B* expression is detected in the developing spiracles.

This is the first report in any chelicerate of coincident anterior boundaries of the three posteriormost Hox genes. These data indicate that the staggered expression of posterior Hox genes previously observed in spiders (Damen et al. 1998; Abzhanov et al. 1999; Schwager et al. 2007) cannot be generalized for the remaining chelicerate orders. Upon comparing spiders and harvestmen, the correlation between expression domains and segmental identities in the opisthosoma suggests the involvement of posterior Hox genes in generating the diversity of the chelicerate opisthosoma.

DISCUSSION

Phalangium opilio as a new model system for study of chelicerate evolution

The aims of this study were to generate comparative data for study of chelicerate development and to assess which aspects of opisthosomal development, including Hox gene expression, are conserved in chelicerates. To this end, we chose the order Opiliones for several reasons. First, harvestmen are distantly related to both tetrapulmonates (the division of arachnids that includes spiders and bears four pairs of opisthosomal organs) and acaromorphs (the clade that includes mites, ticks, and Ricinulei [hooded tick spiders]; Fig. 1), being more closely related to scorpions (Giribet et al. 2002; Shultz 2007). They are therefore exemplars of a plesiomorphic lineage that has been infrequently represented in developmental studies of chelicerates (Popadic and Nagy 2001; Simonnet et al. 2004, 2006). Second, the morphology of harvestmen is evolutionarily conserved, bearing a single pair of opisthosomal organs on an otherwise homonomous and fully segmented opisthosoma in the adults of all species. Finally, certain species of Opiliones are quite amenable to study of development in the laboratory, as they are communal, lay synchronous clutches of eggs, lay multiple clutches per season, and develop almost as rapidly as *A. tepidariorum* (Juberthie 1964). We therefore selected *P. opilio*, a hardy and synanthropic species, for the present investigation.

Anterior Hox gene boundaries reflect conservation of the chelicerate prosoma

Comparison of Hox gene expression in spiders, the mite *A. longisetosus*, and the harvestman *P. opilio* indicates that many aspects of prosomal development are conserved in chelicerates. In all three lineages, the cheliceral segment, which constitutes the deutocerebral segment homologous to the antennal segment of mandibulate arthropods, is free of Hox gene expression (Fig. 9). The anteriormost Hox expression domain commences with the pedipalpal segment in both spiders and *P. opilio*; a *lab* homolog is known to occur in mites, but its expression domain has not been reported (Cook et al. 2001; Grbic et al. 2011). We note that in pycnogonids, *lab* and *pb* are similarly expressed in and posterior to the pedipalpal segment, consistent with previous interpretations of the homology of chelicerae, chelifores, and antennae (Jager et al. 2006; Brenneis et al. 2008). Anterior boundaries of Hox genes expressed in the prosoma are highly conserved in

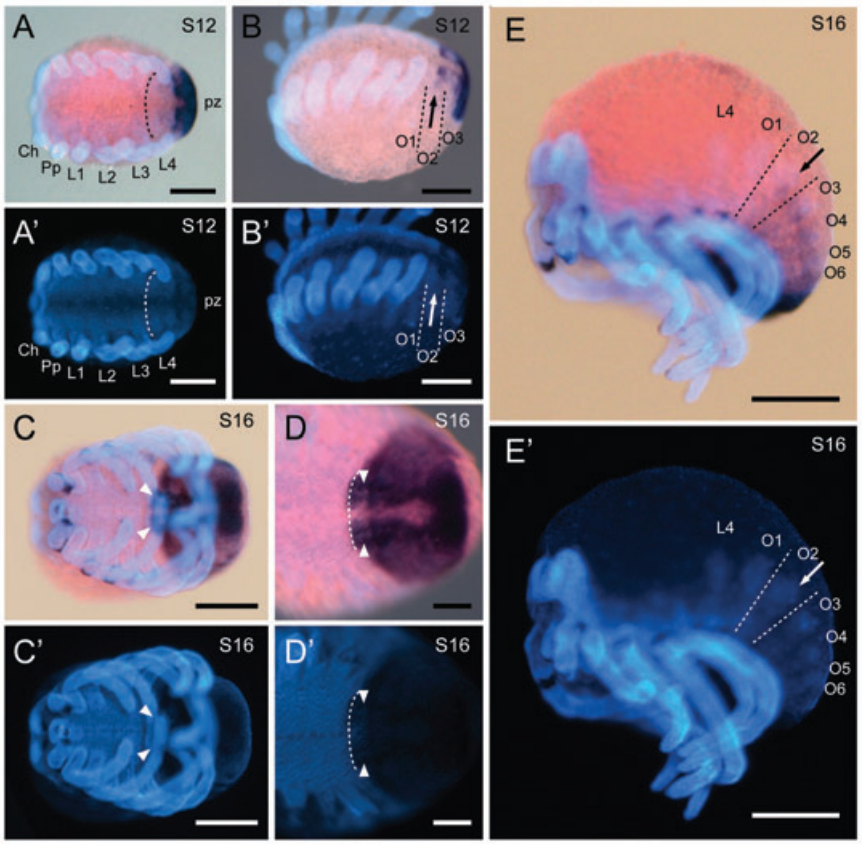

Fig. 7. Expression of the *Phalangium opilio Ultrabithorax* gene. (A) Stage 12 embryo. *Po-Ubx* is expressed strongly in the posterior growth zone, with the anterior boundary of expression occurring in the O2 segment. Dashed line indicates posterior boundary of O1. (B) Same embryo as in (A) in ventrolateral view. Dashed lines indicate boundaries of O2 segment. The anterior boundary of *Po-Ubx* occurs in the middle of the O2 segment, corresponding to the parasegment boundary (arrow). (C) Stage 16 embryo. The anterior boundary of *Po-Ubx* expression is delimited by the expression domain surrounding the genital pores (arrowheads). (D) Detail of *Po-Ubx* expression in the ventral midline of the O2 segment in a stage 16 embryo, with legs excised for clarity. *Po-Ubx* expression is not observed in the pregenital (O1) segment. Dashed line indicates anterior boundary of O2. Arrowheads indicate genital pores on O2. (E) Same embryo as in (C) in lateral view. Expression of *Po-Ubx* is clearly observed in the posterior part of the O2 segment. Dashed lines indicate anterior and posterior boundary of O2. Arrow indicates anterior boundary of *Po-Ubx* expression in lateral aspect. Note the nonspecific staining in the distal tips of the chelicerae and the bases of the appendages due to cuticle deposition in (C) and (E). (A'–E') Counterstaining of embryos shown in (A–E) with Hoechst. Scale bars are 100 μm for (D) and (D'), and 200 μm for all others. Abbreviations are as in Fig. 2.

the three lineages. These data are consistent with the observation that the six-segmented arachnid prosoma is a highly conserved structure, much like the archetypal configuration of the mandibulate head in myriapods and pancrustaceans (Telford and Thomas 1998a; Hughes and Kaufman 2002a).

Posterior Hox gene domains reflect evolutionary changes in opisthosomal morphology

In contrast to the prosoma, the chelicerate opisthosoma is evolutionarily a far more labile tagma in both embryo and adult. *Apropos*, the posterior Hox gene expression patterns observed in spiders appear to be correlated with the configuration and identity of the opisthosomal organs specific to this order (Fig. 9). By contrast, within Acari (mites and ticks), some lineages have demonstrably lost true segmentation of the opisthosoma altogether. Consistent with this morphology, developmental study of two mite species has revealed that only two anterior opisthosomal segments express the conserved segment polarity gene *engrailed*, and the posterior Hox gene *abd-A* has been lost altogether (Grbic et al. 2011; A. A. Barnett and R. H. Thomas, pers. comm.). Finally, harvestmen bear a single pair of respiratory organs and the genital pores on the O2 segment, on an otherwise homonomous opisthosoma; the anterior boundaries of the three posteriormost Hox genes are coincident and occur in the O2 segment in *P. opilio*. These data suggest a correlation between the anterior boundaries of the posteriormost three Hox genes and the fate of the opisthosomal segments they pattern.

Evolution of the anterior boundary of *Ubx* has been examined in several other chelicerates, including a xiphosuran, a scorpion, and three spiders (Damen et al. 1998; Abzhanov et al. 1999; Popadic and Nagy 2001). Together with these data, the expression domain of *Po-Ubx* corroborates the observation that, in contrast to crustaceans, changes in the embryonic expression of *Ubx* are not correlated with changes in adult morphology of chelicerates (Popadic and Nagy 2001). How then is the diversity of the chelicerate opisthosoma patterned?

One possibility may be that changes in the expression domains of *abd-A* and *Abd-B* enable the morphological

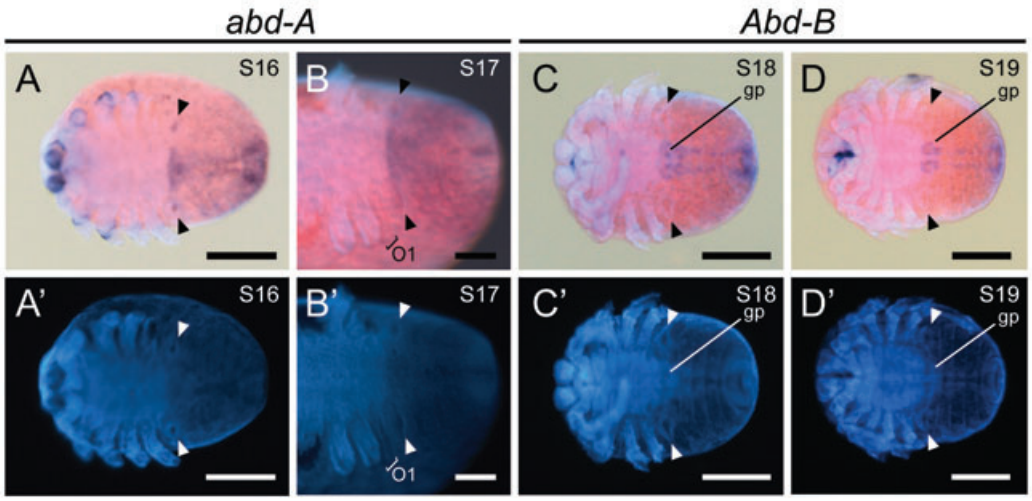

Fig. 8. Expression of the *Phalangium opilio abdominal-A* and *Abdominal-B* genes. (A) Stage 16 embryo. *Po-abd-A* is expressed from the O2 segment to the posterior growth zone. Expression is observed around the genital pores and in the spiracles, which occur on the O2 segment but are laterally displaced from the ventral midline. The strongest expression occurs in the posterior growth zone. Arrowheads indicate spiracles on O2. (B) Stage 17 embryo. *Po-abd-A* expression is more diffuse, but is still observed in the O2 segment around the genital pores and throughout the posterior opisthosomal segments. Bracket indicates O1, which becomes smaller during embryogenesis and is not observed as a full segment in the adult. Arrowheads indicate spiracles on O2. (C) Stage 18 embryo. *Po-Abd-B* expression is observed in the ventral ectoderm from O2 to the posterior growth zone. Distinct expression domains occur in the developing genital pores on the O2 segment, with an additional ring of expression encircling them. Arrowheads indicate spiracles on O2. (D) Stage 19 embryo. *Po-Abd-B* expression encircles the genital pores. Expression continues to occur in the ventral ectoderm of the opisthosomal segments posterior to O2. Arrowheads indicate spiracles on O2. Note the nonspecific staining in the distal tips of the chelicerae and the bases of the appendages due to cuticle deposition in (A–D). (A'–D') Counterstaining of embryos shown in (A–D) with Hoechst. In all embryos, legs have been excised for clarity. Scale bars are 100 μm for (B) and (B'), and 200 μm for all others. gp: genital pore, all other abbreviations are as in Fig. 2.

variability of the chelicerate opisthosoma. In *P. opilio*, the coincident anterior boundaries of the Hox genes *Ubx*, *abd-A*, and *Abd-B* could resemble a primitive condition of the opisthosoma with respect to both the adult morphology and embryonic development. This postulate would suggest the hypothesis that the co-occurrence of these genes patterns the homonomy of the chelicerate opisthosoma. A corollary of this hypothesis is that the heteronomy of the spider opisthosoma is patterned by the staggered anterior boundaries of the posterior Hox genes. For example, overlapping expression of *Antp* and *Ubx* alone could pattern the respiratory structures on O2 and O3, whereas expression of *Antp*, *Ubx*, and *abd-A* (and possibly weak expression of *Abd-B*) together could pattern the spinnerets on O4 and O5. In both spiders and *P. opilio*, it is the segments that always strongly express all four posterior Hox genes that are homonomous, being neither reduced (as in O1) nor bearing specialized structures (such as genitalia, respiratory organs, or spinnerets).

Further evidence for this hypothesis includes the Hox gene expression domains of *Ubx* and *abd-A* in centipedes (*Lithobius atkinsoni* and *Strigamia maritima*; Hughes and Kaufman 2002b; Brena et al. 2006) and a millipede (*Glomeris marginata*; Janssen and Damen 2006), which overlap almost completely throughout the homonomous trunk segments, much as in the *P. opilio* opisthosoma. A similar phenomenon has been reported for the patterning of the crustacean thorax. In the branchiopod *Artemia franciscana*, *abd-A* expression overlaps almost completely with *Ubx*, from the T2 segment through the entire thorax; in the *Artemia* adult, the thorax is undifferentiated (Averof and Akam 1995). By contrast, in the isopod *Porcellio scaber*, *abd-A* is expressed in the pleon and does not overlap with *Ubx*, which is expressed in the leg-bearing pereon (Abzhanov and Kaufman 2000a). In the decapod *Procambarus clarkii*, the *Ubx* and *abd-A* expression domains roughly correspond to the division between the pereon and the pleon in early stages, and are largely nonoverlapping in late stages (Abzhanov and Kaufman 2000b). It was therefore proposed that the diversification of pancrustaceans was propagated by the subdivision of the expression domains of the four posterior Hox genes, which putatively overlapped completely in the pancrustacean and/or mandibulate ancestor (Averof and Akam 1995; Abzhanov and Kaufman 2000a). The extension of this model to chelicerates was previously hindered by limitations of posterior Hox gene expression data to spider species. Our data suggest that the same dynamic of at least *abd-A*, and possibly *Abd-B* as well, may have driven the diversification of the chelicerate opisthosoma.

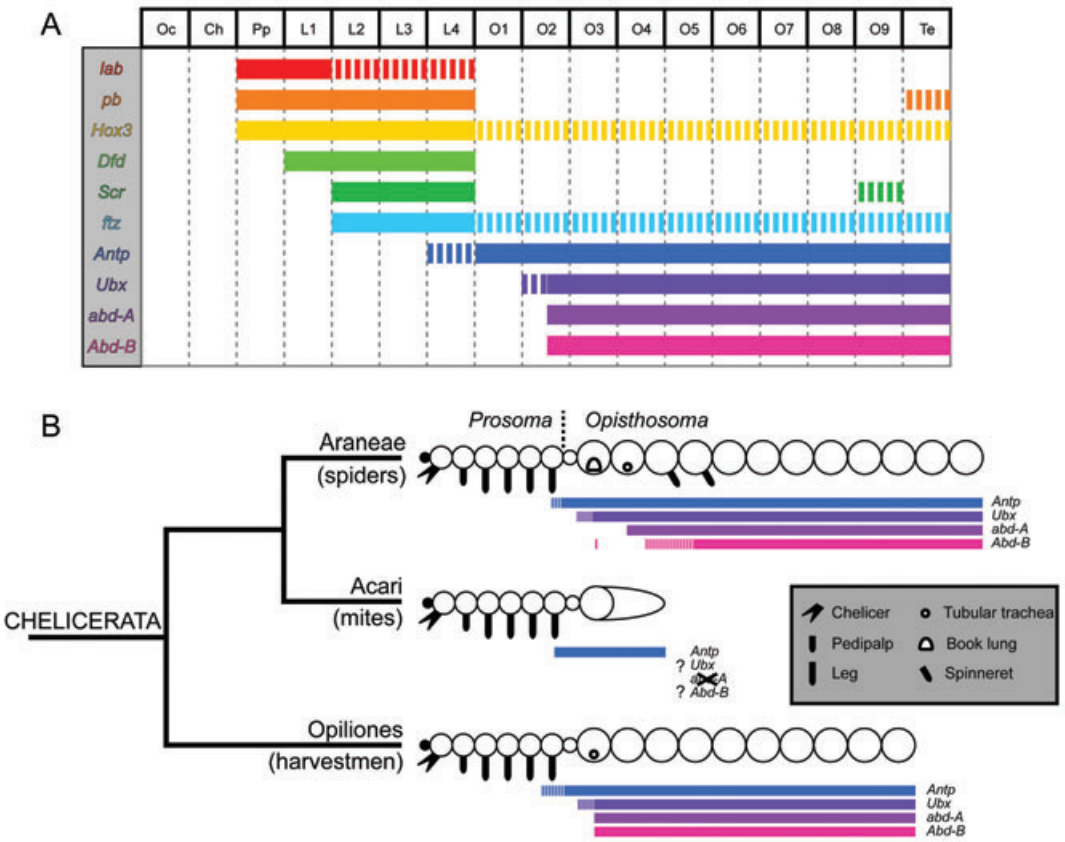

Fig. 9. Summary and comparison of Hox gene expression profiles. (A) Hox gene expression in *Phalangium opilio* for comparison of domain boundaries and correlation with segments. Stripes indicate transient expression (i.e. expansion of an expression domain in later embryonic stages). (B) Comparison of known posterior Hox gene expression domains among chelicerates. Strikethrough of *abd-A* in Acariformes indicates gene loss. Stripes indicate transient expression, as in (A). Multiple colors in the spider indicate differential spatial expression of paralogs. Xiphosura and Scorpiones, for which only *Ubx* has been observed, are not shown. Tagmatic boundary of chelicerates is indicated for the spider.

Abd-B has multiple functions, one of which is patterning of genital structures (Damen and Tautz 1999; Estrada and Sánchez-Herrero 2001; Hughes and Kaufman 2002a). As in *P. opilio*, expression of *Abd-B* in spiders occurs in the genital pores on the O2 segment, but also from the O3 segment to the posterior growth zone (Damen and Tautz 1999). Comparable expression of *Abd-B* does not occur in the geophilomorph centipede *S. maritima* or the millipede *G. marginata*; in these two epimorphic species, *Abd-B* is restricted to the posterior of the embryo, though the genital structures do not occur there in *Glomeris*. However, *Abd-B* is broadly expressed throughout most of the trunk segments in the anamorphic centipede *Lithobius*, much like in spiders and harvestmen (Hughes and Kaufman 2002a, 2002b). The role of *Abd-B* in the O3 and posterior opisthosomal (i.e. nongenitalic) segments is unknown in spiders, and RNAi-mediated knockdown has not been reported. Thus, the anterior boundaries of both *abd-A* and *Abd-B* may be involved in demarcating the part of the opisthosoma in chelicerates that does not bear appendages, such as book lungs and spinnerets.

To further strengthen this correlation, future studies should describe opisthosomal Hox gene domains in other chelicerate orders that have varying suites of opisthosomal organs (e.g. pseudoscorpions have three pairs of respiratory organs; scorpions have four pairs of respiratory organs on the O3–O6 segments). Furthermore, a functional test of this hypothesis could be conducted with RNAi-mediated knockdown of *abd-A* and/or *Abd-B* in *P. opilio* to determine whether a heteronomous opisthosomal phenotype would be obtained (e.g. derepressed limb buds, as in the spider upon *Antp* knockdown; Khadjeh et al. 2012). This approach may be possible given present availability of transcriptomic resources for *P. opilio*, but has yet to be attempted. Alternatively, ectopic expression of all four opisthosomal Hox genes throughout the opisthosoma could be pursued in the spider (e.g. by using the *Antp* promoter to drive

expression of *Ubx*, *abd-A*, and *Abd-B* in *A. tepidariorum*) to determine whether a homonomous opisthosomal phenotype resembling that of *P. opilio* could be recovered. However, such a misexpression system requires the establishment of transgenic lines, a technique of interest that is not currently available for spiders.

CONCLUSION

The tractability and plesiomorphic morphology of *P. opilio* make this species an excellent candidate for generating comparative data on chelicerate morphology, and for anchoring results of other arachnid models—which appear much more derived phylogenetically. Here, we examined gene expression of the single-copy orthologs of all 10 Hox genes in the harvestman. Our results demonstrate that opisthosomal patterning is different among Opiliones and Araneae, and suggest that the unique deployment of Hox genes in *Phalangium* may have a role in the homonomous segmentation of the harvestmen opisthosoma. These results are also predictive of the variability of posterior Hox gene expression throughout other chelicerate orders, which have heretofore not been investigated, in a manner corresponding to their various opisthosomal morphologies.

Acknowledgments

We are indebted to Sónia Andrade, Ana Riesgo, and Alicia Pérez-Porro for technical assistance with the transcriptome of *P. opilio*. Discussions with Austen Barnett, Ariel Chipman, Arkhat Abzhanov, and Andrew H. Knoll refined some of the ideas presented. Dave Smith and Bernhard Götze at the Harvard Center for Biological Imaging facilitated training and use of microscopes. Alysha Heimberg and April Dinwiddie assisted with collections of *P. opilio* in Woods Hole, Falmouth, MA. EES was supported by DFG fellowship SCHW 1557/1-1. Editor Lisa M. Nagy and two anonymous reviewers improved an earlier version of the manuscript. This work was partially supported by NSF grant IOS-0817678 to CGE, and by internal MCZ funds to GG.

REFERENCES

Abzhanov, A., and Kaufman, T. C. 2000a. Crustacean (malacostracan) Hox genes and the evolution of the arthropod trunk. *Development* 127: 2239–2249.

Abzhanov, A., and Kaufman, T. C. 2000b. Embryonic expression patterns of the Hox genes of the crayfish *Procambarus clarkii* (Crustacea, Decapoda). *Evol. Dev.* 2: 271–283.

Abzhanov, A., Popadic, A., and Kaufman, T. C. 1999. Homeotic genes and the arthropod head: expression patterns of the *labial*, *proboscipedia*, and *Deformed* genes in crustaceans and insects. *Proc. Natl. Acad. Sci. USA* 96: 10224–10229.

Akiyama-Oda, Y., and Oda, H. 2003. Early patterning of the spider embryo: a cluster of mesenchymal cells at the cumulus produces Dpp signals received by germ disc epithelial cells. *Development* 130: 1735–1747.

Allard, C. M., and Yeargan, K. V. 2005. Effect of diet on development and reproduction of the harvestman *Phalangium opilio* (Opiliones: Phalangiidae). *Environ. Entomol.* 34: 6–13.

Anderson, D. T. 1973. *Embryology and Phylogeny in Annelids and Arthropods*. Pergamon Press, Oxford, UK.

Angelini, D. R., Liu, P. Z., Hughes, C. L., and Kaufman, T. C. 2005. Hox gene function and interaction in the milkweed bug *Oncopeltus fasciatus* (Hemiptera). *Dev. Biol.* 287: 440–455.

Averof, M., and Akam, M. 1995. Hox genes and the diversification of insect and crustacean body plans. *Nature* 376: 420–423.

Averof, M., and Patel, N. H. 1997. Crustacean appendage evolution associated with changes in Hox gene expression. *Nature* 388: 682–686.

Brena, C., Chipman, A. D., Minelli, A., and Akam, M. 2006. Expression of trunk Hox genes in the centipede *Strigamia maritima*: sense and anti-sense transcripts. *Evol. Dev.* 8: 252–265.

Brenneis, G., Ungerer, P., and Scholtz, G. 2008. The chelifores of sea spiders (Arthropoda, Pycnogonida) are the appendages of the deutocerebral segment. *Evol. Dev.* 10: 717–724.

Carroll, S. B. 1995. Homeotic genes and the evolution of arthropods and chordates. *Nature* 376: 479–485.

Castresana, J. 2000. Selection of conserved blocks from multiple alignments for their use in phylogenetic analysis. *Mol. Biol. Evol.* 17: 540–552.

Cisne, J. L. 1974. Evolution of the world fauna of aquatic free-living arthropods. *Evolution* 28: 337–366.

Cook, C. E., Smith, M. L., Telford, M. J., Bastianello, A., and Akam, M. 2001. Hox genes and the phylogeny of the arthropods. *Curr. Biol.* 11: 759–763.

Damen, W. G. M., Hausdorf, M., Seyfarth, E.-A., and Tautz, D. 1998. A conserved mode of head segmentation in arthropods revealed by the expression pattern of Hox genes in a spider. *Proc. Natl. Acad. Sci. USA* 95: 10665–10670.

Damen, W. G. M., Janssen, R., and Prpic, N.-M. 2005. Pair rule gene orthologs in spider segmentation. *Evol. Dev.* 7: 618–628.

Damen, W. G. M., Saridaki, T., and Averof, M. 2002. Diverse adaptations of an ancestral gill: a common evolutionary origin for wings, breathing organs, and spinnerets. *Curr. Biol.* 12: 1711–1716.

Damen, W. G. M., and Tautz, D. 1998. A hox class 3 orthologue from the spider *Cupiennius salei* is expressed in a Hox-gene-like fashion. *Dev. Genes Evol.* 208: 586–590.

Damen, W. G. M., and Tautz, D. 1999. *Abdominal-B* expression in a spider suggests a general role for *Abdominal-B* in specifying the genital structure. *J. Exp. Zool.* 285: 85–91.

Denell, R. E., Hummels, K. R., Wakimoto, B. T., and Kaufman, T. C. 1981. Developmental studies of lethality associated with the *Antennapedia* gene complex in *Drosophila melanogaster*. *Dev. Biol.* 81: 43–50.

Dunlop, J. A. 1998. The origins of tetrapulmonate book lungs and their significance for chelicerate phylogeny. In *Proceedings of the 17th European Colloquium of Arachnology*, Edinburgh, P. A. Selden (ed), pp 9–16. British Arachnological Society, Buckinghamshire, UK.

Dunn, C. W., et al. 2008. Broad phylogenomic sampling improves resolution of the animal tree of life. *Nature* 452: 745–749.

Edgar, R. C. 2004. MUSCLE: multiple sequence alignment with high accuracy and high throughput. *Nucleic Acids Res.* 32: 1792–1797.

Estrada, B., and Sanchez-Herrero, E. 2001. The Hox gene *Abdominal-B* antagonizes appendage development in the genital disc of Drosophila. *Development* 128: 331–339.

Farley, R. D. 2001. Development of segments and appendages in embryos of the desert scorpion *Paruroctonus mesaensis* (Scorpiones: Vaejovidae). *J. Morphol.* 250: 70–88.

Foelix, R. F. 1996. *Biology of Spiders*, 2nd Ed. Oxford University Press, New York.

Giribet, G., and Edgecombe, G. D. 2012. Reevaluating the arthropod tree of life. *Ann. Rev. Entomol.* 57: 167–186.

Giribet, G., Edgecombe, G. D., and Wheeler, W. C. 2001. Arthropod phylogeny based on eight molecular loci and morphology. *Nature* 413: 157–161.

Giribet, G., Edgecombe, G. D., Wheeler, W. C., and Babbitt, C. 2002. Phylogeny and systematic position of Opiliones: a combined analysis of chelicerate relationships using morphological and molecular data. *Cladistics* 18: 5–70.

González-Reyes, A., and Morata, G. 1990. The developmental effect of overexpressing a *Ubx* product in *Drosophila* embryos is dependent on its interactions with other homeotic products. *Cell* 61: 515–522.
Grbic, M., et al. 2011. The genome of *Tetranychus urticae* reveals herbivorous pest adaptations. *Nature* 479: 487–492.
Hansen, H. J., and Sørensen, W. 1904. *On Two Orders of Arachnida: Opiliones, Especially the Suborder Cyphophthalmi, and Ricinulei, Namely the Family Cryptostemmatoidae*. Cambridge University Press, Cambridge.
Hejnol, A., et al. 2009. Assessing the root of bilaterian animals with scalable phylogenomic methods. *Proc. R. Soc. Lond. B* 276: 4261–4270.
Hughes, C. L., and Kaufman, T. C. 2002a. Hox genes and the evolution of the arthropod body plan. *Evol. Dev.* 4: 459–499.
Hughes, C. L., and Kaufman, T. C. 2002b. Exploring the myriapod body plan: expression patterns of the ten Hox genes in a centipede. *Development* 129: 1225–1238.
Jager, M., Murienne, J., Clabaut, C., Deutsch, J., Le Guyader, H., and Manuel, M. 2006. Homology of arthropod anterior appendages revealed by Hox gene expression in a sea spider. *Nature* 441: 506–508.
Janssen, R., and Damen, W. G. M. 2006. The ten *Hox* genes of the millipede *Glomeris marginata*. *Dev. Genes Evol.* 216: 451–465.
Jones, D., Taylor, W., and Thornton, J. 1992. A new approach to protein fold recognition. *Nature* 358: 86–89.
Juberthie, C. 1964. *Recherches sur la biologie des Opilions*. Dissertation, Université de Toulouse, Toulouse, France.
Khadjeh, S., et al. 2012. Divergent role of the Hox gene *Antennapedia* in spiders is responsible for the convergent evolution of abdominal limb repression. *Proc. Natl. Acad. Sci. USA* 109: 4921–4926.
Lewis, D. L., DeCamillis, M., and Bennett, R. L. 2000. Distinct roles of the homeotic genes *Ubx* and *abd-A* in beetle embryonic abdominal appendage development. *Proc. Natl. Acad. Sci. USA* 97: 4504–4509.
Lewis, E. B. 1978. A gene complex controlling segmentation in *Drosophila*. *Nature* 276: 565–570.
Liubicich, D. M., et al. 2009. Knockdown of *Parhyale Ultrabithorax* recapitulates evolutionary changes in crustacean appendage morphology. *Proc. Natl. Acad. Sci. USA* 106: 13892–13896.
Lynch, J. A., Peel, A. D., Drechsler, A., Averof, M., and Roth, S. 2010. EGF signaling and the origin of axial polarity among the insects. *Curr. Biol.* 20: 1042–1047.
Mann, R. S., and Hogness, D. S. 1990. Functional dissection of *Ultrabithorax* proteins in *Drosophila melanogaster*. *Cell* 60: 597–610.
Manuel, M., Jager, M., Murienne, J., Clabaut, C., and Le Guyader, H. 2006. Hox genes in sea spiders (Pycnogonida) and the homology of arthropod head segments. *Dev. Genes Evol.* 216: 481–491.
Maxmen, A., Browne, W. E., Martindale, M. Q., and Giribet, G. 2005. Neuroanatomy of sea spiders implies an appendicular origin of the protocerebral segment. *Nature* 437: 1144–1148.
Meusemann, K., et al. 2010. A phylogenomic approach to resolve the arthropod tree of life. *Mol. Biol. Evol.* 27: 2451–2464.
Pavlopoulos, A., et al. 2009. Probing the evolution of appendage specialization by Hox gene misexpression in an emerging model crustacean. *Proc. Natl. Acad. Sci. USA* 106: 13897–13902.
Popadic, A., Abzhanov, A., Rusch, D., and Kaufman, T. C. 1998. Understanding the genetic basis of morphological evolution: the role of homeotic genes in the diversification of the arthropod bauplan. *Int. J. Dev. Biol.* 42: 453–461.
Popadic, A., and Nagy, L. 2001. Conservation and variation in *Ubx* expression among chelicerates. *Evol. Dev.* 3: 391–396.
Prpic, N. -M., Schoppmeier, M., and Damen, W. G. M. 2008. Whole-mount in situ hybridization of spider embryos. *CSH protocols* 3(10), pdb.prot5068.
Pultz, M. A., Diederich, R. J., Cribbs, D. L., and Kaufman, T. C. 1988. The *proboscipedia* locus of the Antennapedia complex: a molecular and genetic analysis. *Genes. Dev.* 2: 901–920.
Regier, J. C., et al. 2008. Resolving arthropod phylogeny: exploring phylogenetic signal within 41 kb of protein-coding nuclear gene sequence. *Syst. Biol.* 57: 920–938.
Regier, J. C., et al. 2010. Arthropod relationships revealed by phylogenomic analysis of nuclear protein-coding sequences. *Nature* 463: 1079–1084.
Schwager, E. E., Schoppmeier, M., Pechmann, M., and Damen, W. G. M. 2007. Duplicated hox genes in the spider *Cupiennius salei*. *Front. Zool.* 4: 10.
Shultz, J. W. 1993. Muscular anatomy of the giant whipscorpion, *Mastigoproctus giganteus* (Arachnida, Uropygi), and its evolutionary significance. *Zool. J. Linn. Soc.* 108: 335–365.
Shultz, J. W. 2007. A phylogenetic analysis of the arachnid orders based on morphological characters. *Zool. J. Linn. Soc.* 150: 221–265.
Simonnet, F., Célérier, M.-L., and Quéinnec, E. 2006. *Orthodenticle* and *empty spiracles* genes are expressed in a segmental pattern in chelicerates. *Dev. Genes Evol.* 216: 467–480.
Simonnet, F., Deutsch, J., and Quéinnec, E. 2004. hedgehog is a segment polarity gene in a crustacean and a chelicerate. *Dev. Genes Evol.* 214: 537–545.
Stamatakis, A. 2006. RAxML-VI-HPC: maximum likelihood-based phylogenetic analyses with thousands of taxa and mixed models. *Bioinformatics* 22: 2688–2690.
Telford, M. J. 2000. Evidence for the derivation of the *Drosophila fushi tarazu* gene from a Hox gene orthologous to lophotrochozoan *Lox5*. *Curr. Biol.* 10: 349–352.
Telford, M. J., and Thomas, R. H. 1998a. Expression of homeobox genes shows chelicerate arthropods retain their deutocerebral segment. *Proc. Natl. Acad. Sci. USA* 95: 10671–10675.
Telford, M. J., and Thomas, R. H. 1998b. Of mites and *zen*: expression studies in a chelicerate arthropod confirm *zen* is a divergent Hox gene. *Dev. Genes Evol.* 208: 591–594.
Ueno, K., Hui, C. C., Fukuta, M., and Suzuki, Y. 1992. Molecular analysis of the deletion mutants in the E homeotic complex of the silkworm *Bombyx mori*. *Development* 114: 555–563.
Vachon, G., Cohen, B., Pfeifle, C., McGuffin, M. E., Botas, J., and Cohen, S. M. 1992. Homeotic genes of the bithorax complex repress limb development in the abdomen of the *Drosophila* embryo through the target gene *Distal-less*. *Cell* 71: 437–450.
Wolff, C., and Hilbrant, M. 2011. The embryonic development of the central American wandering spider *Cupiennius salei*. *Front. Zool.* 8: 15.
Yang, Z. 1996. Among-site rate variation and its impact on phylogenetic analyses. *Trends. Ecol. Evol.* 11: 367–372.
Zheng, Z., Khoo, A., Fambrough, D., Garza, L., and Booker, R. 1999. Homeotic gene expression in the wild-type and a homeotic mutant of the moth *Manduca sexta*. *Dev. Genes Evol.* 209: 460–472.

SUPPORTING INFORMATION

Additional Supporting Information may be found in the online version of this article:

Fig. S1. Hox gene tree inferred from maximum likelihood analysis of conserved regions (68 amino acid characters), using selected arthropod taxa for which gene expression has been studied ($\ln L = -1996.476$).

Table S1. List of primer sequences used for riboprobe synthesis.

Supplementary Text. Hox gene alignments.

Please note: Wiley-Blackwell are not responsible for the content or functionality of any supporting materials supplied by the authors. Any queries (other than missing material) should be directed to the corresponding author for the article.